ELSEVIER

Journal of Hazardous Materials B101 (2003) 65–77

Journal of Hazardous Materials

www.elsevier.com/locate/jhazmat

Immobilization of mercury and zinc in an alkali-activated slag matrix

Guangren Qian [a,*], Darren Delai Sun [b], Joo Hwa Tay [b]

[a] *School of Environment Engineering, Shanghai University, No. 149, Yanchang Rd., 200072 Shanghai, PR China*
[b] *Environmental & Engineering Research Centre, School of Civil and Environment Engineering, Nanyang Technological University, Singapore, Singapore*

Received 25 July 2002; received in revised form 14 April 2003; accepted 22 April 2003

Abstract

The behavior of heavy metals mercury and zinc immobilized in an alkali-activated slag (AAS) matrix has been evaluated using physical property tests, pore structure analysis and XRD, TG-DTG, FTIR and TCLP analysis. Low concentrations (0.5%) of mercury and zinc ions had only a slight affect on compressive strength, pore structure and hydration of AAS matrixes. The addition of 2% Hg ions to the AAS matrix resulted in a reduction in early compressive strength but no negative effects were noticed after 28 days of hydration. Meanwhile, 2% Hg ions can be effectively immobilized in the AAS matrix with the leachate meeting the USEPA TCLP mercury limit. For a 2% Zn-doped AAS matrix, the hydration of the AAS paste was greatly retarded and the zinc concentration in the leachate from this matrix was higher than 5 mg/l even at 28 days. Based on these results, we conclude that the physical encapsulation and chemical fixation mechanisms were likely to be responsible for the immobilization of Hg ions in the AAS matrix while only chemical fixation mechanisms were responsible for the immobilization of Zn ions in the AAS matrix.

Keywords: Immobilization; Alkali-activated slag; Mercury; Zinc; Hydration product

1. Introduction

Mercury and zinc are very toxic heavy metals, and are listed as priority pollutants by the USEPA. Solidification /stabilization (s/s) is one of the most important techniques for treating wastes containing mercury, zinc and other heavy metal contaminants. Ordinary Portland cement (OPC) has been the most common solidification materials, because the

* Corresponding author. Fax: +86-21-56333052.
E-mail address: grqian@mail.shu.edu.cn (G. Qian).

0304-3894/03/$ – see front matter © 2003 Elsevier Science B.V. All rights reserved.
doi:10.1016/S0304-3894(03)00143-2

OPC matrix is both economic and effective in chemically immobilizing heavy metals [1,2]. However, high porosity and poor durability of the OPC solidification matrix have been of concern and many modifications to the OPC matrix have been patented and reported [3].

An alkali-activated slag (AAS) matrix is a non-traditional solidifying material, which is made from 100% granulated blast furnace slag and sodium silicate activator. The binding properties of this matrix rely on the alkali activation of aluminosilicate materials. The slag in the AAS matrix reacts with a soluble sodium silicate activator to produce poorly crystallized calcium silicate hydrate C–S–H [4,5]. In the OPC matrix, C–S–H has exhibited a very high immobilization potential for heavy metals [6,7]. Compared to the OPC matrix, the AAS matrix has a higher gel pore volume and a lower capillary pore fraction. The AAS matrix has been successfully utilized in the immobilization of radioactive Sr and Cs wastes [8]. For this reason, the AAS matrix can also be expected to be a good medium for solidifying heavy metals.

Knowledge of the behavior of mercury and zinc in the AAS matrix is scarce, but relevant research on the OPC matrix has been extensively reported. For the Hg-doped OPC matrix, physical precipitation was considered to be the controlling mechanism for the immobilization of mercury, in which the mercury salts tend to hydrolyze to form a red precipitate of HgO in an alkali hydroxide solution or cementious environment [9,10]. However, Poon and Perry [11] and Poon et al. [12] established that a combination of the chemical and physical isolation processes should be utilized for the containment of mercury.

For the Zn-doped OPC matrix, the soluble zinc salt easily exists as zinc hydroxy anions $Zn(OH)_3^-$ and $Zn(OH)_4^{2-}$ in a high pH aqueous environment [13]. These zinc hydroxy anions are transformed into the calcium zincate phase $CaZn_2(OH)_6{\cdot}2H_2O$ which completely covers the cement grains and thus inactivates them from further hydration [2,14]. Mollah et al. [15] suggested that the formation of calcium zincate controls the solubility of zinc. The Zn fixation mechanism for low concentrations differs from those for high concentrations. In the case of low concentrations, zinc ions are nearly incorporated into the C–S–H without other products [16]. The incorporation may either be due to replacement of Ca^{2+} [6] or be a link directly to the end of the silicate chains through Zn–O–Si bonds [16,17].

The AAS matrix is quite different from the OPC matrix. Exploring the immobilizing behavior of mercury and zinc in the AAS matrix has been an objective in many studies. This paper will discuss the affect of mercury and zinc salts on the hydration products, mechanical properties and microstructures of an AAS matrix.

2. Method

2.1. Materials and immobilization matrixes

The blast furnace slag used for the AAS matrix was from Malaysia. Its chemical composition was: 40.31% CaO, 34.47% SiO_2, 9.47% Al_2O_3, 0.53% Fe_2O_3 and 7.81% MgO. It had a specific surface of 480 m^2/kg. All the pastes of the solidification matrix were prepared using a blended alkali solution/slag mass ratio of 0.3. The SiO_2/Na_2O mass ratio of blended

alkali solution was kept at 2.0. This solution was made using sodium silicate solution (with weight ratio of $SiO_2/Na_2O = 2.4$) and NaOH. Five immobilizing matrixes, i.e. pure AAS matrix, 0.5% Hg-AAS, 2% Hg-AAS, 0.5% Zn-AAS and 2% Zn-AAS, were made. Chemically pure $HgNO_3 \cdot H_2O$ and $Zn(NO_3)_2 \cdot 6H_2O$ were added to a sodium silicate solution as sources of Hg or Zn ions, respectively. The amount of Hg ions or Zn ions was determined by weighing the dry slag. The size of cube for compressive strength test was 50 mm. All specimens were cured at room temperature and 100% relative humidity in the incubator for 1, 3, 7, 14 and 28 days.

2.2. Physical tests

The setting time of paste was in accord with ASTM C191-2001. After the specimens were cured for certain periods, the compressive strength was measured according to ASTM C109-2001.

2.3. Leaching test

The TCLP test was conducted using USEPA method EPA-1311 to evaluate the leaching behavior of Hg or Zn ions in the AAS matrixes. After the strength test, the coarse particles were separated by a 9.5 mm sieve. Fifty grams of particle samples were weighed into a 1000 ml polypropylene plastic bottle containing 1000 ml of dilute acetic acid (pH = 2.85) solution. The suspension was shaken for 18 h on an end-over-end shaker at a speed of 30 rpm. The suspension was then filtered. The Hg ion concentrations in the filtered solution were measured by flow injection mercury system (FIMS) and Zn ion concentrations were detected by inductively coupled plasma emission spectrometer(ICP-OES).

2.4. Characterization of hydration products

After a strength test for the cubic specimens, the specimens were crushed into coarse particles or powders and treated with an acetone–alcohol solution to prevent further hydration. XRD, DSC, TG, FTIR and SEM methods were used for identifying the hydration products.

The pore size distribution of matrixes was determined utilizing Micromeritics Autopore III 9400 porosimeter. This device is capable of pressures from 0 to 414 MPa. A hydraulic pump generates the pressure and contact sensor measures the mercury volume. The assumed surface tension of the triple-distilled mercury was 0.484 N/m at 25 °C. The assumed contact angle was 130°.

3. Results and discussion

3.1. Setting time and compressive strength

Pure AAS paste usually has a quicker setting than the OPC paste. Fig. 1 shows the setting time of AAS paste added with mercury or zinc salts. The control sample (pure AAS paste)

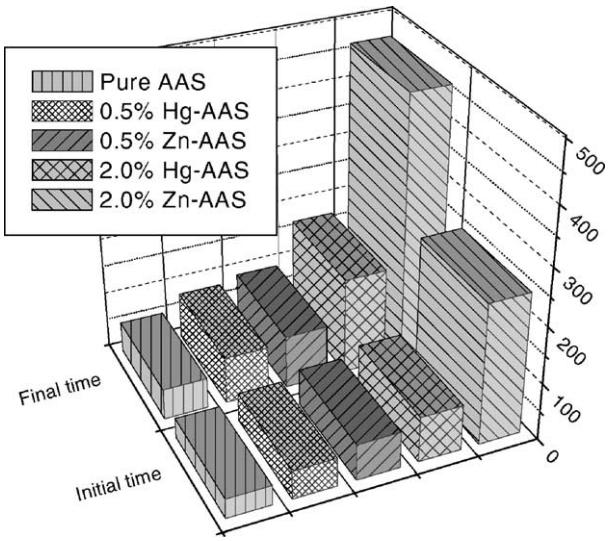

Fig. 1. The setting times (min) of AAS matrixes doped with Hg or Zn ions.

started initial setting within 35 min and got to final setting at 54 min. When mercury or zinc nitrate was added, the setting time of the AAS paste was affected. The degree to which it was affected was highly sensitive to both heavy metal species and ion concentrations. The addition of 0.5% Hg ions or 0.5% Zn ions slightly prolonged the setting time of paste. A 0.5% Hg-AAS paste had a 50 min initial setting time and 82 min final setting time, which was nearly the same as that for 0.5% Zn-AAS paste. For the 2% Hg-AAS paste, however, the initial setting increased to 80 min and final setting was 170 min. Compared with Hg effect, adding 2% Zn ions resulted in more significant retardation on the setting of AAS paste. It had a 248 min initial setting and 467 min final setting time.

The compressive strength also depended on species of heavy metal and its ion concentrations. As seen in Fig. 2, the control sample had a 55.1 MPa of compressive strength at 3 days. The 0.5% Hg-AAS matrix had a 15% strength loss at 3 days relative to the control sample. For a 2% Hg-AAS matrix, a quite poor strength, 2.5 MPa at 3 days, was observed. The compressive strengths of Hg-doped AAS matrix however rose substantially with increased curing time. The strength of 2% Hg-AAS matrix was enhanced to 49.7 MPa at 7 days. At 28 days, all the Hg-doped AAS matrixes had excellent compressive strength, ranged between 70 and 75 MPa. These results suggest that the compressive strength development of Hg-doped AAS pastes at later periods was not affected by Hg additions.

The effects of Zn additions on the compressive strength differed from that of Hg additions. The compressive strengths of a 0.5% Zn-AAS matrix were 38.9–59.6 MPa from 3 to 28 days, which were 15–20% lower than that of the 0.5% Hg-AAS matrix. The 2% Zn-AAS matrix had a quite poor compressive strength of 2–3 MPa from 7 to 14 Days and 9.5 MPa at 28 days. These data imply that the matrix only possesses 13% of compressive strength of pure AAS matrix at 28 days.

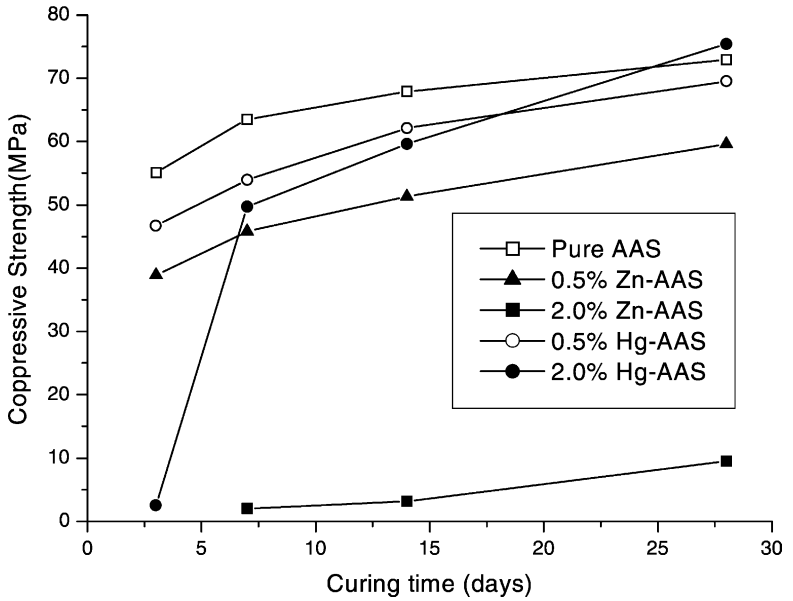

Fig. 2. Compressive strengths of AAS matrixes with different concentrations of Hg or Zn ions plotted as a function of curing time.

3.2. Pore structures

The total porosity and pore size distribution is an important indicator for evaluating the mechanical properties and leaching potential of the solidification matrix. Fig. 3 shows pore

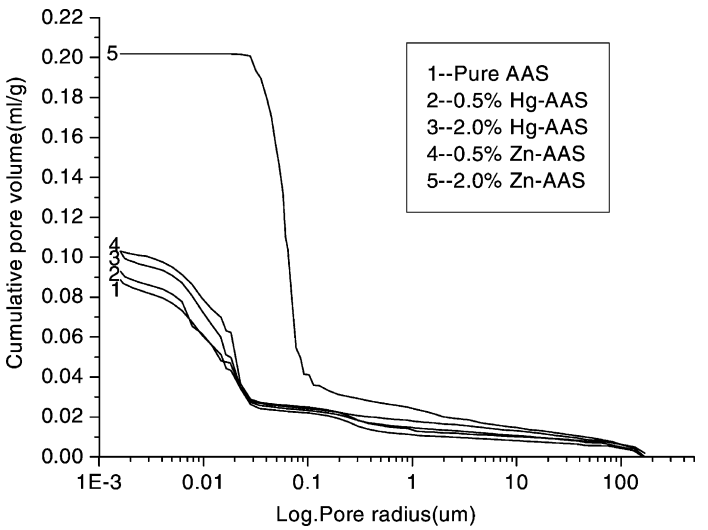

Fig. 3. Cumulative pore size distribution of AAS matrixes doped with Hg or Zn ions.

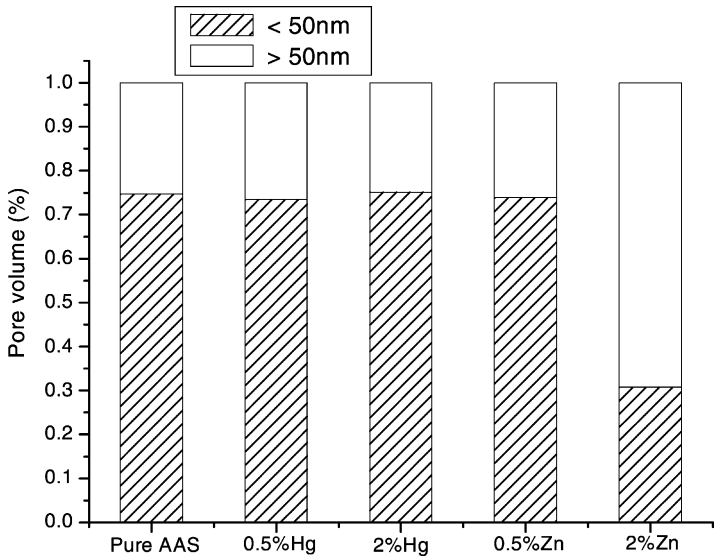

Fig. 4. Mesopore and micropore distribution of AAS matrixes doped with Hg or Zn ions.

size distributions of Hg-doped and Zn-doped AAS matrixes, which were cured for 28 days. Three AAS matrixes, 0.5% Hg-AAS, 2% Hg-AAS and 0.5% Zn-AAS, had similarly shaped pore size distribution as pure AAS matrix and they all had approximately 11% total pore volume. Only the 2% Zn-AAS matrix had a 20% of total pore volume. Moreover, the shape of pore size distribution for 2% Zn-AAS matrix was much different from that of the 0.5% Zn-AAS matrix.

Goto and Roy [18] and Metha [19] suggested that pores larger than 50–100 nm may be detrimental to strength and permeability. Pores less than 50 nm in size are somewhat equivalent to the mesopore defined by IUPAC classification (International Union of Pure and Applied Chemistry) [20]. Based on this concept, Fig. 4 gives quantitative results of pore distribution. A Hg-doped AAS matrix, irrespective of whether 0.5 or 2% Hg was added, had a very close mesopore (<50 nm) volume, of approximately 75%. This mesopore volume was nearly the same as that of pure AAS matrix. This result indicates that the pore refinement of AAS matrix was not affected by Hg additions at 28 days and mesopore predominated over the pore structure of Hg-doped AAS matrixes.

A 0.5% Zn-AAS matrix had a mesopore volume of 74%, which is very close to that of a pure AAS matrix. For a 2% Zn-AAS matrix, the volume of the mesopore was only 31% at 28 days. That finding means that the micropore (>50 nm) predominated over the pore structure of 2% Zn-AAS matrix through its hardening process.

3.3. Leaching behavior

USEPA criteria mandate that the leaching of Hg ions into TCLP extracts must be less than 200 μg/l or the waste is considered as a hazardous waste. Table 1 lists the TCLP leaching

Table 1
Leaching from Hg-doped AAS matrix and Zn-doped AAS matrix by TCLP tests

Curing time (days)	Leaching of Hg (μg/l)		Leaching of Zn (mg/l)	
	0.5% Hg	2% Hg	0.5% Zn	2% Zn
1	1486	4553	81.49	1870.32
3	832	7695	13.42	1954.15
7	317	848	1.18	673.72
14	145	383	0.042	44.78
28	21	65	0.029	9.06

results of Hg-doped AAS matrixes. There is a considerable amount of Hg^{2+} leached from 1 to 7 days for all the Hg-doped AAS matrixes. All values were above the 200 μg/l Hg^{2+} limit given in the TCLP regulation. After curing for 14 days, the Hg^{2+} leached from 0.5% Hg-AAS matrix decreased to 145 μg/l while 2% Hg-AAS matrix still had a Hg^{2+} leachate of 383 μg/l. It was only at 28 days that the Hg^{2+} leaching from 2% Hg-AAS matrix could meet TCLP mercury limit.

The leached Zn ion concentrations in TCLP extracts for Zn-doped AAS matrixes are also listed in Table 1. A 0.5% Zn-AAS matrix cured for 3 days had a Zn^{2+} leachate of 13.42 mg/l; when cured for 7 days, this concentration was down to 1.18 mg/l, far below 5 mg/l limit. In the case of 2% Zn addition, the leachate of matrix cured for 3 days was as high as 1954 mg/l, and decreased to 674 and 45 mg/l at 7 and 14 days, respectively. Even at 28 days, the 2% Zn-AAS matrix had a leachate of 9 mg/l, still much higher than 5 mg/l limit. Although the leachate from the 2% Zn-AAS matrix at 28 days cannot meet TCLP threshold limit, over 99.99% Zn ions had been fixed in the AAS matrix.

3.4. Hydration products

Physical properties and microstructures of AAS matrixes doped with heavy metals are controlled by the hydration process and reaction products, all of which can be well identified by TG-DTG, DSC, FTIR and SEM methods.

3.4.1. TG and DSC analysis

For a pure AAS matrix, calcium silicate hydrate C–S–H is generally considered to be its major hydration product [4]. Fig. 5 shows DSC curves of hydration products for Hg or Zn-AAS matrixes. Like a pure AAS matrix, other AAS matrixes with Hg or Zn addition yielded a steeper endothermic peak around 130 °C and a broad exothermal peak at 770–850 °C when cured for 28 days; these results suggest a gradual dehydration of the C–S–H interlayer and the decomposition of C–S–H into wollastonite. The exothermal peak of pure AAS matrix was at 820 °C. With the increase of Hg ions in the AAS matrix, this exothermal peak was shifted toward higher temperature, 832 °C for 0.5% Hg and 842 °C for 2% Hg. However, Zn-doped matrixes had an opposite shift tendency towards a lower temperature, 815 °C for 0.5% Zn and 775 °C for 2% Zn. Diamond et al. [21] proved that the position shift of exothermal peak produced by C–S–H was related to the incorporation of other ions in the lattice of C–S–H.

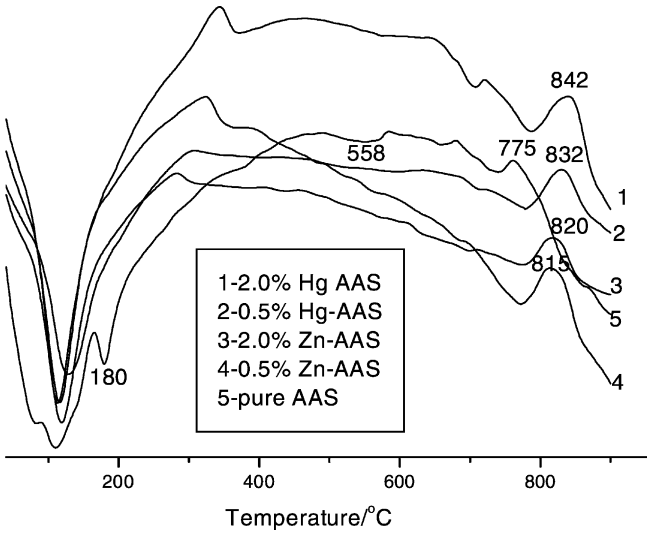

Fig. 5. DSC curves of AAS matrixes doped with Hg or Zn ions.

Amorphous metal silicate is supposed to be another reaction product. Iler [22] reported that polyvalent metal salts easily react with soluble silicates to produce insoluble amorphous metal silicate precipitates formed by adsorption on gelatinous silica. The existence of an amorphous metal silicate precipitate in the AAS matrix with heavy metals could be detected by thermal analysis. Maliavski et al. [23] found that metal orthosilicate gel had a significant thermal decomposition in the 300–580 °C temperature range. As shown in Fig. 6, 2% Hg-AAS matrix had a trough of derivate weight loss around 466 °C; As for the 2% Zn-AAS matrix, not only two troughs of derivate weight loss at 398 and 535 °C, respectively, but also a poor endothermic peak around 558 °C in Fig. 5 could be observed. Judged by Maliavski's results, above troughs of derivate weight loss and poor endothermic peak should be proof of the existence of amorphous mercury silicate or zinc silicate precipitate.

Two new phases could be identified by thermal analysis when 2% Hg or 2% Zn ions were added to the AAS matrix. One phase results from the formation of HgO in the 2% Hg-AAS matrix. The 2% Hg-AAS matrix showed a steep weight loss with DTG peak centered at 302 °C (Fig. 6). Ortego et al. [9] attributed this additional weight loss to the decomposition of HgO into volatile elemental mercury and oxygen. The other new phase is the formation of calcium zincate $CaZn_2(OH)_6{\cdot}2H_2O$ in the 2% Zn-AAS matrix. The 2% Zn-AAS matrix gave a significant weight loss with DTG peak centered at 161 °C in Fig. 6 and a steep endothermic peak at 180 °C in Fig. 5. Ubbriaco et al. [24] attributed these results to the decomposition of calcium zincate phase.

Additionally, the effect of Hg or Zn ions on the hydration of AAS matrix could be evaluated by the TG method. As shown in Fig. 6, the weight loss of all the samples was nearly a constant value at approximately 700 °C, at which chemically combined water in the AAS matrixes was fully lost. Thus, the magnitude of weight loss at 700 °C in TG curves can be used as an approximate estimation of chemical combined water. This transformation

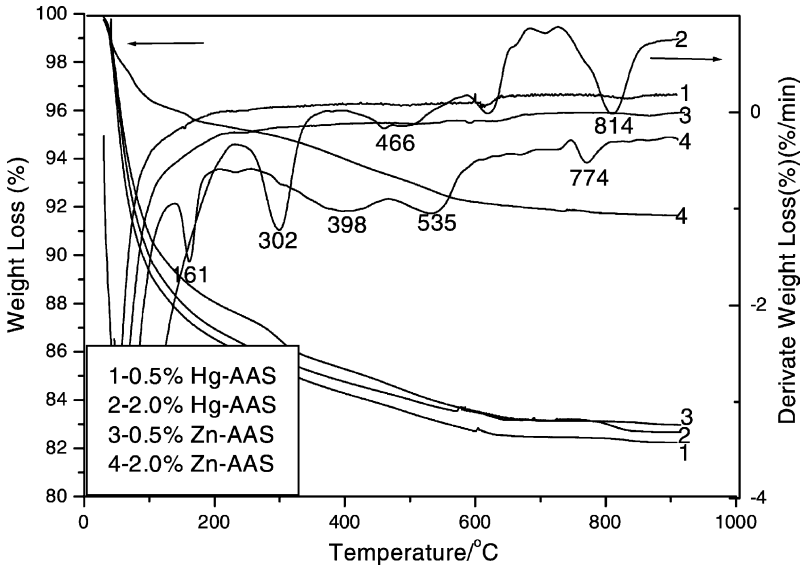

Fig. 6. TG-DTG curves of AAS matrixes doped with Hg or Zn ions.

should be related to the hydration degree of the AAS matrixes. By observation, three AAS matrixes cured for 28 days—0.5% Hg-AAS, 2% Hg-AAS and 0.5% Zn-AAS matrix—had nearly the same weight loss, meaning that they had an approximate hydration degree at 28 days. The case for 2% Zn-AAS matrix was an exception. Its weight loss at 28 days was only about one half of 0.5% Zn-AAS matrix. These results are identical with the compressive strength of AAS matrix with heavy metals. They support the contention that additions of Hg ions have no negative effect on the later hydration of Hg-AAS paste while effects of Zn ions highly depend on its concentrations.

3.4.2. FTIR

The FTIR results also proved the existence of C–S–H hydration product. As shown in Fig. 7, there two absorption bands appeared at 3470–3450 and 1655–1640 cm^{-1} in all the samples. These bands are, respectively, due to stretching and deformation vibrations of OH and H–O–H groups from and water molecules of C–S–H. There existed another strong absorption band around 1000 cm^{-1}, which is attributed to ν_3 vibration of Si–O–Si asymmetric stretch mode. Considering that amorphous metal silicate precipitate is another reaction product containing Si–O–Si stretch bond besides C–S–H [24], this absorption band around 1000 cm^{-1} should include the contributions from both products. As shown in Fig. 7, the ν_3 band of the AAS matrixes with Hg or Zn additions had a shift toward high wave number relative to pure AAS matrix. Magnitude of the shift seemed to correspond to heavy metal addition. The ν_3 band frequency of pure AAS matrix is 970 cm^{-1}. For the Hg-AAS matrix, this ν_3 band shifted to 973 cm^{-1} (0.5% Hg) and 981 cm^{-1} (2% Hg). In the case of the Zn-AAS matrix, this ν_3 band shifted to 975 cm^{-1} (0.5% Zn) and 1027 cm^{-1} (2%

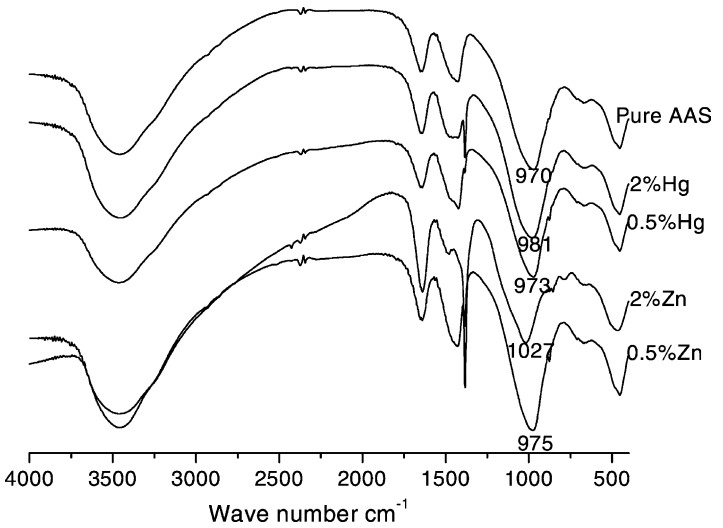

Fig. 7. FTIR spectra of AAS matrixes doped with Hg or Zn ions.

Zn). Previous results [25] established that the ν_3 band of Si–O–Si is sensitive to vibration of linkages between Si–O–Si tetrahedra and surrounding secondary building blocks of the structure. The fact of ν_3 band shift indicates that the Hg or Zn ions possibly acted as secondary building blocks of the structure to modify surrounding linkages of Si–O–Si tetrahedra. These heavy metals might be incorporated into the C–S–H and combined into amorphous metal silicate precipitate rather than just physically encapsulated.

3.4.3. SEM

Fig. 8 shows the morphologies of hydration products for the AAS matrixes with Hg or Zn additions, which were cured for 28 days. As illustrated in Fig. 8a, 2% Hg-AAS matrix produced a lot of fine flake-like hydration products with length of 1–2 μm. These products could be considered as C–S–H. Both 0.5% Hg-AAS and 0.5% Zn-AAS matrixes also had a significant amount of dense and fine flake-like C–S–H products (Fig. 8b). However, the morphology of hydration products for the 2% Zn-AAS matrix was not easily distinguished as an amorphous product layer covered the surface of unreacted particles and there still existed many visible voids among the particles (Fig. 8c). This result supports a finding that the 2% Zn-AAS matrix did not hydrate well even at 28 days.

3.5. Mechanisms of immobilization

Based on TCLP leaching results, we found that Hg and Zn ions could be effectively immobilized in the AAS matrix. As a comparison, the immobilizing efficacies of the AAS matrix on Hg ions were stronger than on Zn ions. Significantly, the physical encapsulation mechanism, in addition to chemical fixation mechanisms, played an important role in the effective immobilization of Hg ions. The contribution of physical encapsulation came from

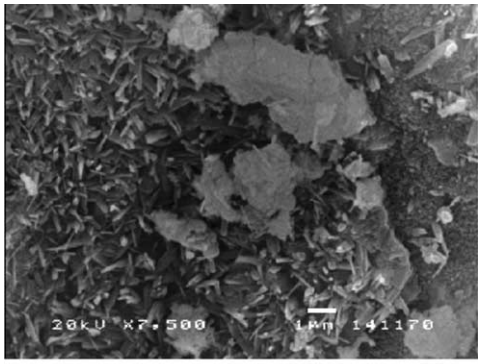

(a)

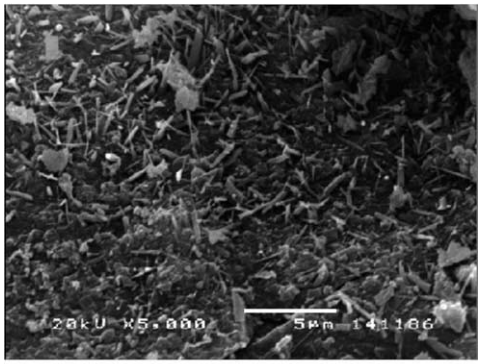

(b)

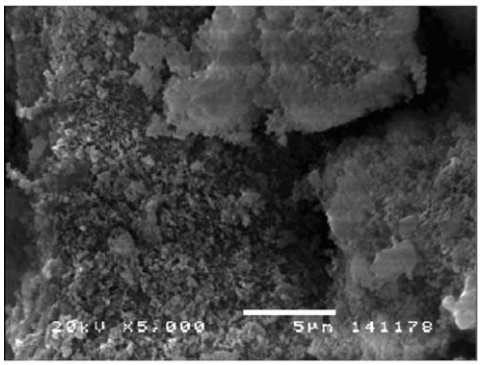

(c)

Fig. 8. Morphology of hydration products for Hg or Zn-doped AAS matrixes at 28 days: (a) 2% Hg-doped AAS matrix; (b) 0.5% Zn(Hg)-doped AAS matrix; and (c) 2% Zn-doped AAS matrix.

refined pore structure of the Hg-doped AAS matrix and filling of amorphous metal silicate precipitates in the pore structure, which prevented less soluble HgO that formed in aqueous environment from physical leaching. However, the 2% Zn-doped AAS matrix had quite a low compressive strength and coarser pore structure. In this case, the physical encapsulation could not be the controlling mechanism for immobilizing Zn ions in the AAS matrix. Alternatively, the chemical fixation mechanisms could be responsible for this effect.

According to an analysis of hydration products, we concluded that the chemical fixation mechanisms for immobilizing Hg or Zn ions in the AAS matrix may include three aspects: (1) the formation of insoluble meal silicate gel such as mercury silicate gel or zinc silicate gel; (2) the formation of less soluble HgO or insoluble calcium zincate precipitate; and (3) the incorporation of metal ions in the lattice of C–S–H. The predominant mechanism depends on both heavy metal concentration and reaction process. A possible assumption is that heavy metal Hg^{2+} or Zn^{2+} was preferentially reacted with soluble silicate to form insoluble amorphous metal silicate precipitates, or competitively, was bound into the crystal lattice of C–S–H as metal salt was added into the AAS paste. After that, free metal ions may react to form less soluble HgO or insoluble calcium zincate precipitate as a physical encapsulation in the aqueous environment. This assumption was supported by two facts. One possibility is that 0.5% Hg-AAS matrix had no HgO formed but C–S–H and mercury silicate gel. The other is that no calcium zincate was found for 0.5% Zn-AAS matrix. For the OPC matrix with low Zn ion concentrations, Rose et al. [16] gave the same evidence that Zn ions were only incorporated in the C–S–H framework without any precipitation products.

However, the exact process of formation of calcium zincate phase, immobilizing mechanisms of Hg-CSH phase and effects of mercury and zinc on the formation of gelatinous precipitate in the AAS matrix are still not clear, more detailed proof is needed.

4. Conclusions

A low concentration (0.5%) of heavy metals Hg and Zn had only a slight affect on the compressive strength, pore structure and hydration of AAS matrixes. Although the addition of 2% Hg ions to the AAS matrix yielded an evident reduction in early compressive strength, no negative effects were noticed after hydration for 28 days. Moreover, 2% Hg ions can be effectively immobilized in the AAS matrix with the leachate meeting the USEPA TCLP mercury limit.

For 2% Zn-doped AAS matrix, even at 28 days, not only was the hydration of AAS paste still greatly retarded but also the leaching from this matrix was still higher than 5 mg/l.

References

[1] F.P. Glasser, in: R.D. Spence (Ed.), Chemistry and Microstructure of Solidified Waste Forms, Lewis Publishers, Florida, 1993, p. 1.

[2] D.L. Cocke, A. Mollah, in: R.D. Spence (Ed.), Chemistry and Microstructure of Solidified Waste Forms, Lewis Publisher, Florida, 1993, p. 187.

[3] J.R. Conner, Chemical Fixation and Solidification of Hazardous Wastes, Van Nostrand Reinhold, New York, 1990.
[4] D.M. Roy, Cem. Concr. Res. 29 (1999) 249.
[5] S.D. Wang, Adv. Cem. Res. 12 (2000) 163.
[6] S. Komarneni, E. Breval, D.M. Roy, R. Roy, Cem. Concr. Res. 8 (1978) 204.
[7] F.P. Glasser, in: T. White, J.A. Stegemann (Eds.), Advances in Environmental Materials, vol. II, Environmental Preferred Materials, Materials Research Society, Singapore, 2001, p. 281.
[8] G.R. Qian, D.D. Sun, J.H. Tay, J. Nucl. Mater. 299 (2001) 199.
[9] J.D. Ortego, S. Jackson, G.S. Yu, H. McWhinney, D.L. Coke, J. Environ. Sci. Health A24 (1989) 589.
[10] H.G. McWhinney, D.L. Cocke, K. Balke, J.D. Ortego, Cem. Concr. Res. 20 (1990) 79.
[11] C.S. Poon, R. Perry, Fly ash and coal conversion by-products characterization, utilization and disposal III, in: G.J. McCarthy, F.P. Glasser, D.M. Roy, S. Diamond (Eds.), Proceedings of the Materials Research Society Symposium, Materials Research Society, Pittsburgh, PA, 1987, p. 67.
[12] C.S. Poon, A.I. Clark, R. Perry, Cem. Concr. Res. 16 (1986) 161.
[13] M. Pourbaix, Atlas of Electrochemical Equilibria in Aqueous Solutions, National Association of Corrosion Engineering, Houston, TX, 1974.
[14] M.Y.A. Mollah, R.K. Vempati, T.C. Lin, D.L. Cocke, Waste Manage. 15 (1995) 137.
[15] M.Y.A. Mollah, J.R. Parga, D.L. Cocke, J. Envir. Sci. Health, Part A 27 (1992) 1503.
[16] J. Rose, I. Moulin, A. Mason, P.N. Bertsch, M.R. Wiesner, J.Y. Bottero, F. Mosnier, C. Haehnel, Langmuir 17 (2001) 3658.
[17] I. Moulin, W.E.E. Stone, J. Sanz, J.Y. Bottero, F. Mosnier, C. Haehnel, Langmuir 15 (1999) 2829.
[18] S. Goto, D. Roy, Cem. Concr. Res. 11 (1981) 75–757.
[19] P.K. Metha, Concrete: Its Structure, Properties and Materials, Prentice-Hall, Englewood Cliffs, NJ, 1986.
[20] IUPAC, J. Pure Appl. Chem. 31 (1978) 578.
[21] S. Diamond, J.J. White, W.L. Dolch, Am. Mineral. 51 (1966) 388.
[22] R.K. Iler, The Chemistry of Silica, Wiley, NY, 1979.
[23] N.I. Maliavski, O.V. Dushkin, G. Scarinci, Ceram. Silik. 45 (2001) 48.
[24] P. Ubbriaco, P. Bruno, A. Traini, D. Calabrese, J. Therm. Anal. Calorim. 66 (2001) 293.
[25] J.S. van Jaarsveld, J.S.J. van Deventer, Cem. Concr. Res. 29 (1999) 1189.